AcetylacetonateBODIPY−biscyclometalated Iridium(III) complexes: Effective strategy towards smarte fluorescentphotosensitizer agents

E. Palao, R. Sola-Llano, A. Tabero, H. Manzano, A. R. Agarrabeitia, A. Villanueva, I. López-Arbeloa, V. Martínez-Martínez, and M. J. Ortiz

http://dx.doi.org/10.1002/chem.201701347

Chem.Eur.J.2017,23,10139–10147

10.1002/chem.201701347

WILEY-VCH

AcetylacetonateBODIPY−biscyclometalated Iridium(III) complexes: Effective strategy towards smarter fluorescent-photosensitizer agents

E. Palao,[a] R. Sola-Llano,[b] A. Tabero,[c] H. Manzano,[d] A. R. Agarrabeitia,[a] A. Villanueva,[c,e] I. López-Arbeloa,[b] V. Martínez-Martínez,*[b] and M. J. Ortiz*[a]

Abstract: Biscyclometalated Ir(III) complexes involving BODIPY-based ancillary ligands, where the BODIPY unit is grafted to different chelating cores (acetylacetonate for **Ir-1** and **Ir-2**, and bipyridine for **Ir-3**) by the BODIPY *meso* position, have been synthesized and characterized. Complexes having the BODIPY moiety directly grafted to acetylacetonate (**Ir-1** and **Ir-2**) exhibit higher absorption coefficient (*ca.* ε = 4.46 10^4 M^{-1} cm^{-1} and 3.38 10^4 $M^{-1}cm^{-1}$ at 517 nm and 594 nm, respectively), higher moderate-fluorescence emission (*ca.* ϕ_{fl} = 0.08 and 0.22 at 528 nm and 652 nm, respectively) and, especially, more efficient singlet oxygen generation upon visible-light irradiation (*ca.* ϕ_{Δ} = 0.86 and 0.59, respectively) than that exhibited by **Ir-3** (*ca.* ϕ_{Δ} = 0.51, but only under UV light). Phosphorescence emission, nanosecond time-resolved transient absorption and DFT calculations suggest that BODIPY-localized long-lived ^{3}IL states are populated for **Ir-1** and **Ir-2**. *In-vitro* photodynamic therapy (PDT) activity studied for **Ir-1** and **Ir-2** in HeLa cells shows that such complexes are efficiently internalized into the cells, exhibiting low dark- and high photo-cytoxicity, even at significant low complex concentration, making them potentially suitable as theranostic agents.

Introduction

Photodynamic therapy (PDT) using singlet oxygen ($^1O_2$) photosensitizer (PS) agents (*i.e.,* dyes able to generate cytotoxic $^1O_2$ under light irradiation) being additionally fluorescence emitters (*i.e.*, PS able to enable imaging capability; fluorescent-PDT agents) are currently undergoing intensive investigations as promising biomaterials for theragnosis.[1] Over the last years, grafting a visible-light-absorbing organic dye to a transition-metal coordination complex has emerged as an attractive way to develop fluorescent-PDT agents.[2,3] Although conceptually inspiring, transition metal complexes showing fluorescence emission together with effective intersystem crossing (ISC) are still at an early stage of development, the major challenge probably being the simultaneous activation of these two photophysically opposed processes under visible (Vis) light. Particularly, many of the research efforts on new photosensitizer based on metal complex are focused on Ir(III), since it is considered to be one of the most inert and stable transition metals, which are two very desirable properties when designing biomaterials.[4] However, although organo-Ir(III) complexes have demonstrated efficient photoinduced $^1O_2$ generation, they mostly show absorption bands only in the ultraviolet (UV) region, with low molar extinction coefficient also.

To overcome this drawback, two molecular-designing strategies have been pursued. On the one hand, most of the investigations are focused on attaching a light-harvesting chromophore to the complex via a π-conjugated linker.[2,3] Among all of them, biscyclometalated Ir(III) complexes (complexes having two metalacycles involving C-Ir bonds) functionalized with a boron-dipyrromethene (BODIPY) unit through a C≡C bond have become promising systems, since they enable modest fluorescence emission with high $^1O_2$ generation quantum yields.[3] On the other hand, simply attaching the Vis-light-absorbing organic ligand to the coordination center has been also explored as a valuable strategy, although this approach has not assured effective funneling of the excitation energy to the triplet excited-state manifold.[2] In spite of the efforts focused on the development of these dye-containing metallic complexes, few of them have proved to be successful enough as to act as efficient fluorescent-PDT agents.

Analyzing the molecular structures of the reported BODIPY dyes (BDP) anchored to cyclometalated complexes, most of them involve pyridine-based ancillary ligands. Nonetheless, other ancillary groups, such as acetylacetonate (acac), have been successfully involved in organometallic derivatives with outstanding behavior as photosensitizers.[2,4b,5] Besides, Prof. Peña-Cabrera *et al.*[6] have demonstrated that the direct incorporation of stabilized-1,3-diketonate nucleophilic groups,

[a] Dr. E. Palao, Prof. Dr. A. R. Agarrabeitia, Prof. Dr. M. J. Ortiz
Departamento de Química Orgánica I
Facultad de Ciencias Químicas
Ciudad Universitaria s/n, 28040, Madrid, Spain
E-mail: mjortiz@ucm.es
[b] Dr. R. Sola-Llano, Prof. Dr. I. López-Arbeloa, Dr. V. Martínez-Martínez
Departamento de Química Física
Universidad del País Vasco-EHU
Apartado 644, 48080, Bilbao, Spain
E-mail: virginia.martinez@ehu.eus
[c] A. Tabero, Prof. Dr. A. Villanueva
Departamento de Biología
Universidad Autónoma de Madrid
Darwin 2, 28049, Madrid, Spain
[d] Dr. Hegoi Manzano
Departamento de Física de la Materia Condensada
Universidad del País Vasco, UPV/EHU
Apartado 644, 48080, Bilbao, Spain
[e] Prof. Dr. A. Villanueva
Instituto Madrileño de Estudios Avanzados (IMDEA) Nanociencia
Ciudad Universitaria de Cantoblanco, 28049, Madrid, Spain

Supporting information for this article is given via a link at the end of the document.

with well-known chelating properties, to the *meso* position of BODIPYs renders dyes with highlighted optical properties, which shows the great importance of establishing new BODIPY post-functionalization strategies.[7] Moreover, such a *meso* functionalization maintains available the 2 and 6 BODIPY positions for further functionalizacion to finely modulate the photophysical properties of the final material (*i.e.*, shifting the absorption to the red by incorporating π-systems).

Attending these precedents, we envisaged a new molecular-designing strategy to develop advanced fluorescent-PDT materials based on acetylacetonated BODIPY chelating biscyclometalated Ir(III) (**Ir-1** and **Ir-2**, Figure 1). To elucidate the relevance of the involved acac moiety, connecting metal and BODIPY, a related iridium complex bearing the same biscyclometalated-Ir(III) and *meso*-substituted BODIPY core, but having a bipyridine-based ligand covalently connected to the BODIPY core through a π-conjugated spacer (**Ir 3** in Figure 1) was also synthesized and studied.

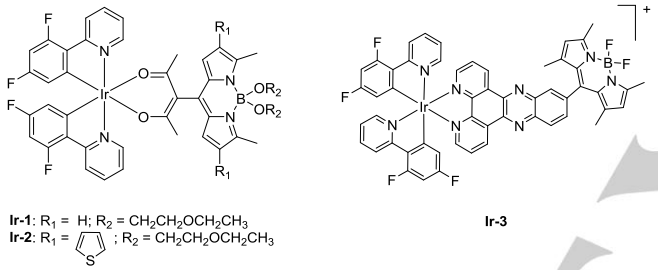

Figure 1. Structures of the iridium complexes.

A comprehensive computationally-aided (DFT) photophysical study, based on conventional steady-state and time-resolved UV-VIS spectroscopies, demonstrates that **Ir-1** and **Ir-2** exhibit an ideal balance between fluorescence emission and $^1O_2$ generation, making them suitable as efficient organometallic fluorescent-PDT agents. Regarding this, conducted *in-vitro* experiments show that these compounds internalize efficiently into HeLa cells, enabling low dark- and high photo-cytoxicity also, even at low concentration, which boots the potential application of the bis(cyclometalated) Ir(III) complexes.

Results and Discussion

Scheme 1 shows the synthesis of the new BODIPY-functionalized bis(cyclometalated) Ir(III) complexes. Acetylacetone-based *meso*-substituted BODIPY **acacBDP-1** was obtained following the procedure described by Peña-Cabrera *et al.*[6] Iodination of **acacBDP-1** with *N*-iodosuccinimide (NIS), followed by Suzuki reaction with 2-thienylboronic acid, affords **acacBDP-2**. Biscyclometalated Ir(III) complexes based on *O*-BODIPY **Ir-1** and **Ir-2** were prepared following the procedure described by Thompson *et al.*,[5b] by reacting dinuclear-complex precursor $[Ir(dfppy)_2Cl]_2$[8] with the corresponding aforementioned acac-based *meso*-substituted BODIPY (Scheme 1). It must be noted here that, under the required reaction conditions not only the desired chelation took place, but also substitution of the BODIPY fluorine atoms by solvent (2-ethoxyethanol) molecules, to afford the final *O*-BODIPY-based complex. This non-projected extra functionalization is interesting, since *O*-BODIPY dyes proved to be highly effective in the development of dyes with enhanced photostability for lasing[9] and with improved water solubility for biology,[10] among other applications.[11].On the other hand, biscyclometalated Ir(III) complex **Ir-3** was obtained by reacting phenantrodione **1** with $[Ir(dfppy)_2Cl]_2$, followed by condensation of the so-obtained complex dione **2** with diaminoBODIPY **3**[12] (Scheme 1).

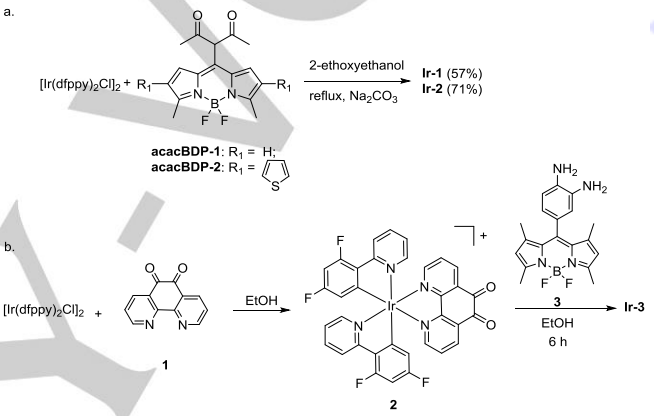

Scheme 1. Synthesis of the iridium complexes; dfppy is the cyclometalating anionic ligand based on 2-(2,4-difluorophenyl)pyridine.

The photophysical properties of the new BODIPY-containing Iridium complexes as well as those of the free acac-BODIPY dyes, analyzed in aerated acetonitrile solutions at room temperature, are summarized in Table 1. The attachment of an acac-BODIPY to Ir(III) via a non-π-conjugated linker does not result in any noticeable electron coupling between moieties, at least in the ground state, since the absorption spectra of the new compounds **Ir-1** and **Ir-2** are roughly the sum of the absorption of each-isolated moiety. That is, **Ir-1** and **Ir-2** exhibit an intense and sharp band centered at 517 and 597 nm (Figure 2), which corresponds to the **acacBDP-1** and **acacBDP-2** units, respectively, together with a low absorption in the UV range characteristic of the organometallic complex without dye (*i.e.* compound **2** in Scheme 1). In this regard, no significant shift of the absorption bands upon complexation with Ir(III) was observed, but molar coefficients (ε) at the maximum absorption ~~has~~ increased up to 8-fold (Table 1) with respect to the electronically-isolated BDP moieties. This enhancement of the absorption capacity could be a consequence of replacing fluorine atoms in the boron center by alkoxy groups.[9]

In spite of the intense fluorescence of the free ligand **acacBDP-1**, scarce fluorescence at room temperature was recorded for the corresponding **Ir-1** complex (Table 1). This remarkable fluorescence quenching should be related to the efficient ISC to the triplet excited state leading to an effective $^1O_2$

generation (86%) upon visible light excitation (Table 1), whereas the **acacBDP-1** free ligand does not enable $^1O_2$ sensitization.

Table 1. Photophysical properties of the free ligands and cyclometalated Ir(III) complexes in aerated acetonitrile solution at room temperature. Absorption (λ_{abs}) and fluorescence (λ_{flu}) wavelengths at the maximum; molar absorption at the maximum (ε_{max}); fluorescence quantum yield (ϕ_{flu}), singlet oxygen generation quantum yield (ϕ_{Δ}).

Compound	λ_{abs} [nm]	ε_{max} [$10^{-4}M^{-1}cm^{-1}$]	λ_{flu} [nm]	ϕ_{flu}	ϕ_{Δ}
acacBDP-1	515	0.99	526	0.90	0
acacBDP-2	600	0.41	677	0.09	0
Ir-1	517	4.46	528	0.08	0.86[a]
Ir-2	597	3.38	652	0.22	0.60[b]
Ir-3	502	2.60	546	0.01	0.51[c]

[a] λ_{exc} = 530 nm (Rose Bengal as reference); [b] λ_{exc} = 605 nm (New methylene blue as reference); [c] λ_{exc} = 370 nm (Phenalenone as reference)

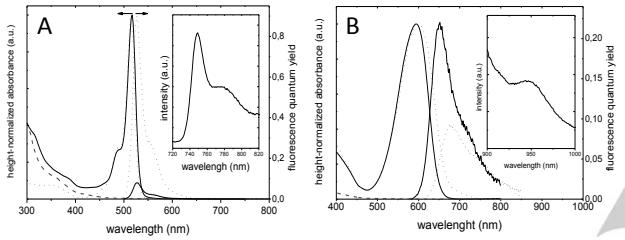

Figure 2. A) Normalized absorption and fluorescence spectra of **Ir-1** (solid lines) and the **acacBDP-1** (dotted curves) and **2** (dashed curve). The phosphorescence band of **Ir-1** measured at 77 K in EtOH is inserted. B) Normalized absorption and fluorescence spectra of **Ir-2** (solid lines) and the **acacBDP-2** (dotted curves) and **2** (dashed curve). The phosphorescence band of **Ir-2** measured at 77 K in EtOH is inserted.

A more interesting feature is the distinct behavior of **Ir-2**. Regarding the chromophoric ligands herein selected, by tethering thienyl-groups on 2 and 6 position of the BODIPY core in **acacBDP-2**, the absorption and fluorescence emission bands are red-shifted, placing both within the spectral region of biological interest. With respect to the free ligand **acacBDP-2**, the fluorescence band of the metallic complex **Ir-2** is blue-shifted by 25 nm and surprisingly the emission efficiency is significantly increased (ϕ_{fl} = 0.22, Table 1). In this regard, the metallic complexation of the free ligand **acacBDP-2** should significantly reduce the geometry relaxation of the 2,6-dithienyl-BODIPY molecular framework after photoexcitation,[13] responsible for large Stokes shifts and considered as the main non-radiative deactivation process in these derivatives. However, the **Ir-2** complex also enables moderate $^1O_2$ photosensitizing ability (ϕ_{Δ} = 0.60) in agreement with its relatively higher emissive efficiency, which is *ca.* 3-fold higher than that of **Ir-1**. In this way, a proper balance between the singlet oxygen generation and fluorescence ability is attained in **Ir-2**.

To shed light on the mechanism of the singlet oxygen generation in these BODIPY-metallic systems the nanosecond time-resolved transient absorption spectra were analyzed. Upon pulsed laser excitation, broad positive transient absorption (TA) bands in the range 400-450 and 600-700 nm were observed for **Ir-1** (Figure S1). The bleaching band for **Ir-1** is located at 517 nm, which is in good agreement with the steady-state absorption spectrum (Figure 2). Regardless of the excitation wavelength, similar decay curves from both TA bands were recorded, leading to a lifetime of 8.4 μs in deaerated solution, which becomes drastically reduced (385 ns) in aerated solutions (Figure S1). The TA spectrum of **Ir-2** is similar to that of **Ir-1**, with the bleaching band centered at 595 nm and positive transient absorptions in the range of 330-480 nm and 655−850 nm (Figure S2). In this case, the lifetime was 9.6 μs in deaerated solution and 480 ns in aerated ones. The spectral signature of both **Ir-1** and **Ir-2** suggests that the long lifetime excited state (~ 10 μs) could be ascribed to the lowest-lying BODIPY-centered triplet (^{3}LC) state.[3b,14] To further analyze the triplet excited state of these BODIPY-containing metallic complexes, the luminescence of the metallic complexes **Ir-1** and **Ir-2** was recorded at 77 K in deaerated ethanolic solutions and compared to that endowed by the own ligand acacBDP-1. Regardless of the excitation wavelength within the range 480-530 nm, where the metal subunit has negligible absorption, Ir-1 exhibits two emission bands: a very intense emission centered at 528 nm, previously assigned to the fluorescence emission of the BODIPY moiety, and a very weak band centered at 749 nm (Figure 2A, inset), with an associated lifetime of 2.4 ms. Similar spectral features are recorded from the ligand acacBDP-1 although its phosphorescence emission intensity is at least 10-fold lower than that registered from the corresponding Ir-1 complex. On the basis of these results, this long-lived emission can be properly assigned to the phosphorescence from the BODIPY unit, which emission intensity becomes significantly enhanced by its attaching to a cyclometalated Ir(III) complex. Regarding **Ir-2**, the phosphorescence band registered at 77 K was placed at long-wavelength, peaked at 948 nm (Figure 2B).

In this sense, two mechanisms have been postulated to promote $^3\pi$-π^* BODIPY level through an effective intersystem crossing after exciting its fluorescent $^1\pi$-π^* state. On the one hand, a photoinduced electron-transfer process from the singlet BODIPY level to the metal complex via an intermediate charge-separated state that would produce the lowest-lying $^3\pi$-π^* state by recombination.[14c,15] On the other hand, the interaction between the BODIPY $^3\pi$-π^* and the closely-lying metal-based ^{3}MLCT level, would provide a channel to enhance spin-orbit coupling in these compounds.[3b,14a] Thus, to indentify the mechanism of the population of the BODIPY triplet state, the photophysical properties of **Ir-2** were theoretically analyzed by density functional theory (DFT) calculations (Figure 3). The optimized ground state geometry of **Ir-2** complex shows that the BODIPY takes a perpendicular orientation with respect to the acetylacetonate linker, so a π-conjugation of the BODIPY and the Iridium center is not expected. On the other hand, the thienyl-groups are perfectly aligned with the BODIPY center, therefore extending the π-conjugated system in agreement with the experimentally observed red-shifted absorption and emission bands.

The UV/Vis absorption and emission of **Ir-2** was studied by Time-dependent density functional theory (TDDFT B3LYP/ LanL2DZ) calculations. The absorption wavelength, calculated

assuming a Franck-Condon vertical transitions, is 564 nm (2.20 eV), smaller but close to the experimental result at 597 nm.

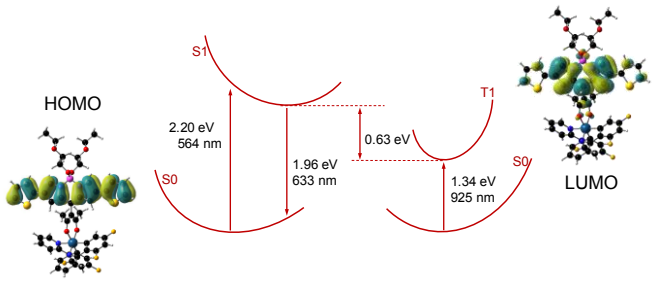

Figure 3. Schematic representation of the photophysical process in the **Ir-2**. Arrows indicate the direction of the transition, with the corresponding energy and wavelength. S_0, S_1, and T_1 states represent the ground state, excited state and triplet state respectively. The spatial location of the HOMO and LUMO atomic orbitals is also included. The detailed ground state geometry and spatial location of the spin density are given in the SI.

The molecular orbitals involved in this $S_0 \rightarrow S_1$ transition are the HOMO and LUMO, both localized in the BODIPY moiety. Notice that both MO are extended through the BODIPY and the thienyl-groups, which confirms the efficient π-conjugation suggested from the ground state geometry. The emission wavelength was calculated after an optimization of the dye excited state conformation. No relevant changes were observed neither in the BODIPY planarity nor in the BODIPY acetylacetonate linker perpendicular arrangement. The emission $S_1 \rightarrow S_0$ emission wavelength is 633 nm (1.96 eV), again slightly lower than the experimental value of 652 nm. The stokes shift predicted by the simulation (69 nm) is therefore in good agreement with the experimental one (55 nm). The HOMO and LUMO orbitals of the optimized excited state are localized as in the ground state geometry, so charge transfer processes could be ruled out.

The adiabatic energy gap between the optimized S_0/T_1 states is 1.34 eV (926 nm), just 1 nm larger than the $S_0 \rightarrow T_1$ wavelength predicted by TDDFT, and in good agreement with the experimental phosphorescence wavelength (948 nm). TDDFT calculations indicate that the involved orbitals are again the HOMO and LUMO, and therefore the T_1 state can be attributed to a BODIPY-centered triplet (^{3}LC) state, as concluded from the nanosecond time-resolved transient difference absorption spectroscopy of this complex.

To complete the theoretical study, we analyzed the localization of the spin density in **Ir-2**. The isosurface map, included in the SI (Figure S3), shows the spin density localized exclusively in the BODIPY unit, in agreement with the previous assignment of triplet state as a ^{3}LC state.

Interestingly, the effective energy funneling to the triplet state manifold in **Ir-1** and **Ir-2** renders a good balance ~~the best balance~~ between fluorescence/$^1O_2$ generation in a common solvent ~~reported up to date from cyclometalated Ir(III) complexes with BODIPY ligands~~. In this regard, Zhao *et al*.[3a] achieved, from complexes based on attaching bulky organic fluorophores to one[3a] or two[3c] coordination centers via π-conjugation linker, quantum yield ratios ranging from 0.06/0.81[3a] to ~~4.7/53~~ 0.25/0.75. [3c] However, the rational design of the complexes herein synthesized, despite being based on a direct and non-conjugated binding of the fluorophore to the metallic center, allows effective visible light absorption and fine-tuning of the photophysical properties of the final material to accomplish dual functionalities giving relatively strong fluorescence efficiency together with high $^1O_2$ photosensitizing ability, *i.e* 0.80/0.86 and 0.22/0.60 for **Ir-1** and **Ir-2**, respectively. These results confirm our initial hypothesis on the key role of acac linkers to promote BODIPY-containing metallic center materials with enhanced properties for advanced applications.

In contrast, the binding strategies followed to date, usually involving π-conjugation linkers, maximize the heavy metal atom effect of the metallic center and, consequently, enhances the singlet oxygen generation in detriment of the emission efficiency. To confirm this behavior, we analyzed the photophysical properties of **Ir-3**, a π-extended metalated Ir(III) complex bearing the same cyclometalating ligands than **Ir-1** but with a bipyridine unit acting as ancillary ligand of the BODIPY moiety. **Ir-3** shows strong absorption in the visible region but its fluorescence is practically quenched ~~but~~ although it is non-effective in generating singlet oxygen species in the visible range (Table 1). That is, moderate $^1O_2$ quantum yield of 51% is achieved only ~~to~~ by directly exciting the metallic center under UV irradiation (Table 1).

The outstanding performance of **Ir-1** and **Ir-2** could be particularly well suited for theragnosis. In this regard, their uptake, as well as, their dark- and photo-cytoxicity was assessed in tumor HeLa cell line. As shown in Figure 4A, **Ir-1** and **Ir-2** internalization into cells was visualized by fluorescence microscopy under blue (460-490 nm) and green (510-550 nm) excitation. Moreover, both compounds exhibit none or minimal toxicity without irradiation (dark toxicity) (Figure 4B) evaluated by MTT assay. [16] However, when incubation was followed by green (for **Ir-1**) or red (for **Ir-2**) light irradiation (6.8 J/cm2), both compounds triggered phototoxicity on cells (see Figure 4C). In our experimental conditions (green excitation centered at 532 nm, and red excitation at 632 nm) compound **Ir-1** showed a significantly higher phototoxicity than **Ir-2**, triggering 50% of cell death at very low concentration (50 nM).

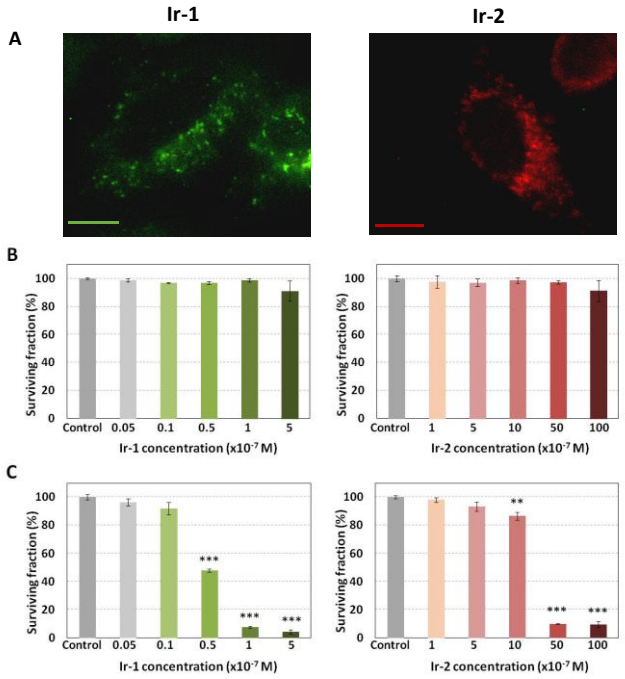

Figure 4. HeLa cells experiments. (A) Internalized **Ir-1** and **Ir-2** compounds detected inside HeLa cells after incubation for 24 h with 5 x 10^{-7} M. Scale bar: 5 μm. (B) Surviving fractions of HeLa cells after 24 h incubation with the compounds at different concentration, in the absence of irradiation (dark toxicity). (C) HeLa cells survival after exposure for 24 h to **Ir-1** or **Ir-2** at different concentrations followed by 6.8 J/cm^2 of green or red light irradiation (for **Ir-1** and **Ir-2**, respectively). Cell viability was evaluated by MTT assay 24 h after each treatment. Data correspond to mean ± S.D. values from at least six different experiments. Statistically significant differences are labeled as * p<0.01 ** p<0.005 *** p<0.001 for comparisons between groups using one-way ANOVA.

Conclusions

In summary, we demonstrate a new molecular-designing strategy to develop smarter fluorescent-PDT materials based on Ir(III) complex. It consists in using easily-accessible *meso*-acetylacetonated BODIPY as anchillary ligand chelating a bis(cyclometalated) Ir(III) center, to obtain a $^1O_2$ PS able to be efficiently triggered with Vis light. In fact, these BODIPY-dyed organometallic compounds demonstrate to internalize well into HeLa cells with low dark-toxicity, but maintaining fluorescence response and photoinduced $^1O_2$-generation, allowing efficient PDT,under Vis light excitation, even at low complex concentration. This behavior overcomes the drawbacks of common iridium-complex PSs with characteristic absorption bands in the UV spectral range.

Experimental Section

General.

Synthesis. All starting materials and reagents were commercially, unless indicated otherwise, and used without further purifications. Common solvents were dried and distilled by standard procedures. Flash chromatography was performed using silica gel (230-400 mesh). NMR spectra were recorded at 20 ºC in $CDCl_3$, using the residual solvent peaks as internal reference. Chemical shift multiplicities are reported as: s = singlet, d = doublet, dd = double doublet, t = triplet, td = triplet of doublets, appt = apparent triplet, q = quartet, m = multiplet. FTIR spectra were obtained from neat samples using the ATR technique. Melting points were determined in open capillaries and are uncorrected. Mass spectrometry (MS) was performed using the FAB$^+$ technique. High resolution mass spectrometry (HRMS) was conducted using the EI and TOF MALDI techniques.

Photophysical properties. Photophysical signatures were measured in diluted solutions (2 x 10^{-6} M) in acetonitrile (spectroscopic grade) and 1 cm path length quartz cuvettes. The absorption spectra were registered in a Varian spectrophotometer (model Cary 4E). The steady-state fluorescence and singlet oxygen emission spectra were recorded in an Edinburgh Instruments spectrofluorimeter (model FLSP920). The emission spectra were corrected from the monochromator wavelength dependence, the lamp profile and the photomultiplier sensitivity. Fluorescence quantum yields (ϕ_{fl}) for compounds **Ir-1**, **Ir-3** and **acacBDP-1** were calculated upon excitation at 490 nm using commercial PM567 (ϕ_{fl}^r = 0.84 in ethanol) as reference, while for the red-edge emitting **Ir-2** and **acacBDP-2**, Nile Blue (ϕ_{fl}^r = 0.12 in ethanol) upon excitation at 590 nm, was considered.

Singlet oxygen production. The production of $^1O_2$ was determined by direct measurement of the luminescence at 1270 nm with a NIR detector integrated in the spectrofluorimeter (InGaAs detector, Hamamatsu G8605-23). The $^1O_2$ signal was registered in front configuration (front face), 40° and 50° to the excitation and emission beams, respectively and leaned 30° to the plane formed by the direction of incidence and registration in cells of 1 cm. The signal is filtered by a low cut-off of 850 nm. $^1O_2$-generation quantum yield (ϕ_Δ) was determined using the following equation:

$$\phi_\Delta = \phi_\Delta^r \cdot (\alpha^r/\alpha_{Ps})\,(Se_{Ps}/Se^r)$$

where ϕ_Δ^r is the quantum yield of $^1O_2$ generation for the used reference (in our case, Rose bengal and new methylene blue). Factor $\alpha = 1\text{-}10^{-Abs}$, corrects the different amount of photons absorbed by the sample (α_{Ps}) and reference (α^r). Factor Se is the intensity of the $^1O_2$ phosphorescence signal of the sample (Se_{Ps}) and the reference (Se^r) at 1276 nm, phenalenone, Rose bengal and new methylene blue in acetonitrile were used as references for UV (370 nm), green (530 nm) and red (610 nm) irradiation, respectively with singlet oxygen quantum yields in acetonitrile of ϕ_Δ^r = 1[17], ϕ_Δ^r = 0.53[18] and ϕ_Δ^r = 0.71 (measured in laboratory of País Vasco University with respect to Rose bengal), respectively. $^1O_2$ quantum yields were averaged at least from 5 air-saturated solutions of concentrations between 6 x 10^{-6} M and 6 x 10^{-5} M in acetonitrile.

Nanosecond time-resolved transient absorption spectroscopy. Nanosecond time-resolved transient difference absorption spectra were recorded on a LP 980 laser flash photolysis spectrometer (Edinburgh Instruments, Livingston, U.K.). Samples were excited by a nanosecond pulsed laser (Nd:YAG laser/OPO, LOTIS TII 2134) operating at 1 Hz at 515 nm for **Ir-1** and 595 nm for **Ir-2**, operating at 1 Hz . The transient signals were recorded on single detector (PMT R928P) and oscilloscope for kinetic traces and ICCD detector DH320T TE cooled (Andor Technology) for time resolved spectra. Data are analyzed by the LP900 software. Samples with an optical absorbance of 0.3 at the excitation wavelength were previously deaerated with argon for ca. 10 min before measurement.

Computational methods. The Gaussian09 code[19] was used for the simulations. In all cases, the DFT simulations were carried out using a B3LYP exchange correlation functional, a LanL2DZ basis set, and a fine integration grid. The ground state and triplet state of the **Ir-2** molecule and the $[Ir(dfppy)_2Cl]_2$ intermediate were optimized, performing a frequency analysis to ensure that the final state was an energy minimum. From the ground state, Franck-Condon vertical transitions to the singlet excited state and the triplet were computed by TDDFT calculation, solving a total of 32 states. The excited state geometry of the **Ir-2** molecule was also optimized in the TDDFT approximation, solving 8 states in this case to obtain emission wavelengths.

Cell cultures. Human cervix adenocarcinoma HeLa cells (ATCC® CCL-2™) were grown as monolayer cultures in Dulbecco's modified Eagle's medium (DMEM) supplemented with 10% (v/v) fetal bovine serum (FBS), 50 U/mL penicillin and 50 µg/mL streptomycin. All products were purchased from Thermo Fisher Scientific (Waltham, MA, USA) and sterilized by means of 0.22 µm filters (Merck Millipore, Billerica, MA, USA). Cell cultures were performed in a 5% CO_2 atmosphere plus 95% air at 37 °C, and maintained in a SteriCult 200 (Hucoa-Erloss, Madrid, Spain) incubator. Subconfluent cell cultures seeded in 24-well plates (with or without coverslip, depending on the experiment) were used. All sterile plastics were from Corning (New York, NY, USA).

Subcellular localization. **Ir-1** and **Ir-2** internalization into HeLa cells was visualized by fluorescence microscopy. Cells were incubated for 24 h with a solution of **Ir-1** or **Ir-2** (5×10^{-7} M) in culture medium (from an initial solution of 2.5×10^{-3} M in dimethyl sulfoxide, DMSO; Panreac, Barcelona, Spain). After incubation with compounds, cells were washed and observed using an Olympus BX61 epifluorescence microscope equipped with an Olympus DP50 digital camera (Olympus, Center Valley, PA, USA) and blue (460-490 nm) and green (510-550 nm) band-pass excitation filters (nm).

Photodynamic treatments. Cells were incubated for 24 h with different concentrations of each compound (diluted in cultured medium from an initial stock 2.5×10^{-3} M in DMSO), washed three times with culture medium without FBS and maintained in culture medium during irradiation and post-treatment time. Irradiations were performed with green (λ_{max} = 518 nm) or red (λ_{max} = 632 nm) light-emitting diode (LED) device (LED Par 64 Short; Showtec, Burgebrach, Holland), to a total light dose of 6.8 J/cm^2 [Total light dose (J/cm^2) = Fluence rate (W/cm^2) x Irradiation time (s)]. Fluence rate (5.7 W/cm^2 for green light and 7.11 W/cm^2 for red light) was measured with the PM100A Handheld Optical Power Meter (Thorlabs, Newton, New Jersey, USA). Besides, experiments with compounds but without irradiation were carried out in order to examine possible dark cytotoxicity. We also checked that this dose of irradiation in the absence of compounds, as well as the % of DMSO present in the 10^{-5} M solution (0.4%), did not have any influence on cell viability (data not shown).

MTT assays. Dark- and photo-toxicity was assessed by MTT colorimetric assay 24 h after treatments. Cells were incubated with a 50 µg/mL solution of 3-(4,5-dimethylthiazol-2-yl)-2,5-diphenyltetrazolium bromide (MTT; Sigma-Aldrich) in culture medium (from an initial MTT stock 1 mg/mL in PBS) for 3 h. Then, reduced formazan was extracted with 500 µL DMSO and absorbance was measured at 542 nm in a SpectraFluor spectrophotometer (Tecan Group Ltd, Männedorf, Switzerland). Cell survival was expressed as the percentage of absorption of treated cells in comparison with that of control cells. Statistical significance for surviving-fraction data acquired from the conducted MTT assays was obtained using one-way ANOVA (all groups vs. control group).

Synthesis and characterization.

$[Ir(dfppy)_2Cl]_2$[8] and compound **acacBDP-1**[6] were synthesized by the corresponding described methods.

acacBDP-2. To a solution of **acacBDP-1**[6] (40 mg, 0.13 mmol) in CH_2Cl_2 (5 mL) was added dropwise a solution of *N*-Iodosuccinimide (NIS) (94 mg, 0.31 mmol) in CH_2Cl_2 (5 mL), and the solution was stirred at room temperature (r. t.) for 4 h. The mixture was washed with water, dried over $MgSO_4$, filtered and concentrated to dryness. Flash chromatography on silica gel using hexane/CH_2Cl_2 (7:3) afforded the diiodinate derivative (44 mg, 61%) as a purple solid.

^{1}H NMR (300 MHz, $CDCl_3$) δ 16.85 (s, 1H, OH), 7.11 (s, 2H, 2CH), 2.64 (s, 6H, $2CH_3$), 2.01 (s, 6H, $2CH_3$) ppm. ^{13}C NMR (75 MHz, $CDCl_3$) δ 191.3 (CO), 160.3, 136.5, 135.2 (CH), 134.6, 106.1, 78.7 (C-I), 24.1 (CH_3), 15.7 (CH_3) ppm. FTIR υ 3113, 2922, 1542, 1423, 1229, 1112, 995 cm^{-1}. EI-HRMS *m/z* 569.9279 (calcd for $C_{16}H_{15}BF_2I_2N_2O_2$: 569.9284).

A solution of diiodinate derivative (40 mg, 0.07 mmol), 2-thienylboronic acid (18 mg, 0.14 mmol), Na_2CO_3 (13.5 mg, 0.14 mmol) and $Pd(PPh_3)_4$ (10%) (8 mg, 0.007 mmol) in DME/H_2O (4:1, 8 mL) was stirred under argon atmosphere at 60 ºC for 60 min. The solvent was then evaporated, and the crude product was dissolved in EtOAc, washed with 10% aqueous HCl, saturated aqueous $NaHCO_3$ and water. The organic layer was dried over $MgSO_4$, filtered and concentrated to dryness. Flash chromatography on silica gel using hexane/EtOAc (9:1) afforded **acacBDP-2** (29 mg, 85%) as a blue solid, mp 224-226 ºC.

^{1}H NMR (300 MHz, $CDCl_3$) δ 16.94 (s, 1H, OH), 7.31 (dd, *J* = 5.1 and 1.2 Hz, 2H, 2CH), 7.14-7.08 (m, 4H, 4CH), 6.95 (s, 2H, 2CH), 2.84 (s, 6H, $2CH_3$), 2.09 (s, 6H, $2CH_3$) ppm. ^{13}C NMR (75 MHz, $CDCl_3$) δ 191.5 (CO), 156.8, 135.5, 135.3, 134.8, 127.8 (CH), 125.0 (CH), 124.8 (CH), 106.7, 24.2 (CH_3), 14.5 (CH_3) ppm. FTIR υ 3101, 2924, 1557, 1434, 1234, 1167 1108, 1009, 982 cm^{-1}. EI-HRMS *m/z* 482.1102 (calcd for $C_{24}H_{21}BF_2N_2O_2S_2$: 482.1106).

Ir-1. $[Ir(dfppy)_2Cl]_2$[8] (38 mg, 0.03 mmol), **acacBDP-1**[6] (20 mg, 0.06 mmol) and Na_2CO_3 (30 mg, 0.31 mmol) in 2-ethoxyethanol (10 mL) were refluxed under argon atmosphere for 5 h. After cooling to r. t., the solvent was evaporated. Flash chromatography on silica gel using CH_2Cl_2/MeOH (98:2) afforded **Ir-1** (37 mg, 57%) as a yellow-brown solid, dec *ca.* 170 ºC

^{1}H NMR (700 MHz, $CDCl_3$) δ 8.55 (d, *J* = 5.6 Hz, 2H, 2CH), 8.33 (d, *J* = 8.4 Hz, 2H, 2CH), 7.90 (appt, *J* = 7.7 Hz, 2H, 2CH), 7.32 (appt, *J* = 6.3 Hz, 2H, 2CH), 6.65 (d, *J* = 4.2 Hz, 2H, 2CH), 6.37 (dd, $^3J_{HF}$ = 10.5 and 9.8 Hz, 2H, 2CH), 6.19 (d, *J* = 4.2 Hz, 2H, 2CH), 5.68 (d, $^3J_{HF}$ = 8.4 Hz, 2H, 2CH), 3.42 (t, *J* = 5.6 Hz, 4H, $2CH_2O$), 3.37 (q, *J* = 7.0 Hz, 4H, $2CH_2O$), 3.07 (t, *J* = 5.6 Hz, 4H, $2CH_2O$), 2.62 (s, 6H, $2CH_3$), 1.72 (s, 6H, $2CH_3$), 1.08 (t, *J* = 7.0 Hz, 6H, $2CH_3$) ppm. ^{13}C NMR (176 MHz, $CDCl_3$) δ 183.8 (CO), 165.6, 162.7 (dd, $^1J_{CF}$ = 255.2 and $^3J_{CF}$ = 14.1 Hz), 160.9 (dd $^1J_{CF}$ = 258.7 and $^3J_{CF}$ = 14.1 Hz), 158.4, 150.8, 147.4 (CH), 141.0, 138.4 (CH), 138.1, 128.5, 126.9 (CH), 123.1 (CH), 123.0 (CH), 121.7 (CH), 119.2 (CH), 115.2 (CH), 115.1 (CH), 107.5, 97.7 (CH), 97.5 (CH), 97.4 (CH), 71.6 (CH_2O), 66.3 (CH_2O), 60.7 (CH_2O), 29.7 (CH_3), 15.2 (CH_3), 15.1 (CH_3) ppm. FTIR υ 2983, 1657, 1566, 1332, 1239, 1150, 976 cm^{-1}. TOF MALDI-HRMS *m/z* calcd for $[C_{46}H_{46}BF_4IrN_4O_6 + H]^+$: 1031.3149, found 1031.3137.

Ir-2. $[Ir(dfppy)_2Cl]_2$[8] (26 mg, 0.02 mmol), **acacBDP-2** (20.6 mg, 0.04 mmol) and Na_2CO_3 (20 mg, 0.46 mmol) in 2-ethoxyethanol (10 mL) were refluxed under argon atmosphere for 2 h. After cooling to r. t., the solvent

was evaporated. Flash chromatography on silica gel using CH_2Cl_2/MeOH (98:2) afforded **Ir-2** (36 mg, 71%) as a blue solid, dec *ca.* 210 ºC.

^{1}H NMR (300 MHz, $CDCl_3$) δ 8.59 (d, J = 4.8 Hz, 2H, 2CH), 8.35 (d, J = 8.7 Hz, 2H, 2CH), 7.92 (dd, J = 7.5 and 6.9 Hz, 2H, 2CH), 7.37 (td, J = 6.0 and 1.2 Hz, 2H, 2CH), 7.31 (dd, J = 4.8 and 1.2 Hz, 2H, 2CH), 7.13-7.07 (m, 4H, 4CH), 6.78 (s, 2H, 2CH), 6.38 (td, $^3J_{HF}$ = 9.0 Hz and J = 2.7 Hz, 2H, 2CH), 5.73 (dd, $^3J_{HF}$ = 8.7 Hz and J = 2.1 Hz, 2H, 2CH), 3.46 (t, J = 5.7 Hz, 4H, $2CH_2O$), 3.37 (q, J = 7.2 Hz, 4H, $2CH_2O$), 3.16 (t, J = 5.7 Hz, 4H, $2CH_2O$), 2.85 (s, 6H, $2CH_3$), 1.79 (s, 6H, $2CH_3$), 1.07 (t, J = 7.2 Hz, 6H, $2CH_3$) ppm. ^{13}C NMR (75 MHz, $CDCl_3$) δ 183.8 (CO), 165.6, 165.5, 162.8 (dd, $^1J_{CF}$ = 254.2 and $^3J_{CF}$ = 12.7 Hz), 161.1 (dd, $^1J_{CF}$ = 257.2 and $^3J_{CF}$ = 15.0 Hz), 156.1, 150.7, 150.6, 147.4 (CH), 140.7, 138.5 (CH), 137.2, 136.7, 127.8 (CH), 126.8, 124.3 (CH), 123.5 (CH), 123.2 (CH), 123.0 (CH), 121.8 (CH), 115.4 (CH), 115.2 (CH), 107.3, 97.9 (CH), 97.6 (CH), 97.2 (CH), 71.5 (CH_2O), 66.3 (CH_2O), 61.0 (CH_2O), 28.9 (CH_3), 15.2 (CH_3), 14.3 (CH_3) ppm. FTIR υ 2974, 1603, 1569, 1403, 1233, 1162, 1100, 987 cm^{-1}. FAB$^+$-MS *m/z* (%) 1194.4 (M^+, 5), 1105.6 (11), 573.5 (100). TOF MALDI-HRMS: *m/z* calcd for $[C_{54}H_{50}BF_4IrN_4O_6S_2+ H]^+$: 1195.2919, found 1195.2903.

Ir-3. $[Ir(dfppy)_2Cl]_2$[8] (60 mg, 0.046 mmol) and 1,10-phenanthroline-5,6-dione (21 mg, 0.1 mmol) in absolute ethanol (10 mL) were refluxed under argon atmosphere for 5 h. After cooling to r. t., the solvent was evaporated and the **2** $[Ir(dfppy)_2(phenO_2)]Cl$ was used for the following synthesis without further purification.

2 (40 mg, 0.06 mmol) and BODIPY **3**[12] in absolute ethanol (20 mL) were refluxed under argon atmosphere for 24 h. After cooling to r. t., the solvent was evaporated. Flash chromatography on silica gel using CH_2Cl_2/MeOH (95:5) afforded **Ir-3** (42 mg, 59%) as a dark red solid, mp > 300 ºC.

^{1}H NMR (700 MHz, $CDCl_3$) δ 9.97 (d, J = 7.7 Hz, 1H, CH), 9.89 (d, J = 7.7 Hz, 1H, CH), 8.62 (d, J = 8.4 Hz, 1H, CH), 8.45 (s, 1H, CH), 8.41 (d, J = 8.4 Hz, 1H, CH), 8.40 (d, J = 9.1 Hz, 1H, CH), 8.32 (t, J = 9.1 Hz, 2H, 2CH), 8.24 (dd, J = 7.7 and 5.6 Hz, 1H, CH), 8.13 (dd, J = 8.4 and 5.6 Hz, 1H, CH), 7.96 (d, J = 8.4 Hz, 1H, CH), 7.81-7.78 (m, 2H, 2CH), 7.75 (d, J = 5.6 Hz, 1H, CH), 7.69 (d, J = 5.6 Hz, 1H, CH), 7.14 (t, J = 7.0 Hz, 1H, CH), 7.10 (t, J = 7.0 Hz, 1H, CH), 6.63 (t, $^3J_{HF}$ = 9.1, 1H, CH), 6.62 (t, $^3J_{HF}$ = 9.1 Hz, 1H, CH), 6.02 (s, 1H, CH), 6.01 (s, 1H, CH), 5.79 (d, $^3J_{HF}$ = 7.7 Hz, 1H, CH), 5.78 (d, $^3J_{HF}$ = 7.7 Hz, 1H, CH), 2.58 (s, 6H, $2CH_3$), 1.33 (s, 3H, CH_3), 1.31 (s, 3H, CH_3) ppm. ^{13}C NMR (75 MHz, $CDCl_3$) δ 164.13, 164.09, 164.0, 163.9, 163.8 (dd, $^1J_{CF}$ = 258.7 Hz and $^3J_{CF}$ = 7.0 Hz, C-F), 163.7 (dd, $^1J_{CF}$ = 258.7 Hz and $^3J_{CF}$ = 7.0 Hz, C-F), 161.5 (dd, $^1J_{CF}$ = 262.2 and $^3J_{CF}$ = 7.0 Hz, C-F), 161.4 (dd, $^1J_{CF}$ = 260.5 and $^3J_{CF}$ = 7.0 Hz, C-F), 156.6, 152.5, 152.4 (CH), 152.3 (CH), 149.7 (CH), 149.4 (CH), 149.2, 142.7, 142.6, 140.5, 140.3, 139.3 (CH), 139.2, 138. 6, 137.0 (CH), 136.8 (CH), 132.5 (CH), 131.6, 131.4, 131.3 (CH), 131.1, 129.6 (CH), 129.0 (CH), 128.6 (CH), 127.7, 127.6, 124.3 (CH), 124.2 (CH), 123.9 (CH), 123.8 (CH), 123.7 (CH), 123.6 (CH), 121.9 (CH), 114.3 (CH), 114.2 (CH), 99.7 (CH), 99.6 (CH), 99.5 (CH), 14.9 (CH_3), 14.7 (CH_3) ppm. FTIR υ 2991, 1542, 1361, 1235, 1130, 989 cm^{-1}. FAB$^+$-MS *m/z* (%) 1101.6 ($[M-Cl^-]^+$, 27), 573.5 (100). TOF MALDI-HRMS *m/z* calcd for $[C_{53}H_{35}BF_6IrN_8]^+$: 1101.2623, found 1101.2615.

Acknowledgements

Financial support from MINECO (MAT2014-51937-C-2-P and 3-P and MAT2015-68837-REDT), MICINN (CTQ2013-48767-C3-3-R), Comunidad de Madrid (S2013/MIT-2850) of Spain and Gobierno Vasco (IT912-16) is gratefully acknowledged. V. M-M. thanks MINECO for a postdoctoral contract (RYC-2011-09505). R.S-L thanks UPV-EHU for a postdoctoral fellowship, and A.T. thanks UAM for a predoctoral contract. The authors thank for technical and human support provided by SGIker of UPV/EHU and European funding (ERDF and ESF).

Keywords: Iridium(III) complex • BODIPYs • singlet oxygen • fluorescent-photosensitizers • photodynamic therapy • HeLa cells.

[1] Selected references: (a) D. García-Fresnadillo, S. Lacombe in *Singlet Oxygen. Applications in Biosciences and Nanosciences*, *Vol. 1* (Eds.: S Nonell, C. Flors) Royal Society of Chemistry, Cambridge, **2016**, Chapter 6, pp. 105-143; (b) K. K. Ng, G. Zheng, *Chem. Rev.* **2015**, *115*, 11012–11042; (c) X. Liu, I. Que, X. Kong, Y. Zhang, L. Tu, Y. Chang, T. T. Wang, A. Chan, C. W. G. M. Löwik, H. Zhang, *Nanoscale* **2015**, *7*, 14914–14923; (d) P. Liu, C. Yue, Z. Sheng, G. Gao, M. Li, H. Yi, C. Zheng, B. Wang, L. Cai, *Polym. Chem*. **2014**, *5*, 874–881; (e) P. Huang J. Lin, X. Wang, Z. Wang, C. Zhang, M. He, K. Wang, F. Chen, Z. Li, G. Shen, D. Cui, X. Chen, *Adv. Mater*. **2012**, *24*, 5104–5110; (f) X. Liang, X. Li, X. Yue, Z. Dai, *Angew. Chem. Int. Ed*. **2011**, *50*, 11622–11627.

[2] Selected reviews: (a) J. Zhao, W. Wu, J. Sun, S. Guo, *Chem. Soc. Rev.* **2013**, *42*, 5323-5351; (b) J. Zhao, S. Ji, W. Wu, W. Wu, H. Guo, J. Sun, H. Sun, Y. Liu, Q. Li, L. Huang, *RSC Adv.* **2012**, *2*, 1712-1728 and references cited therein.

[3] (a) P. Majumdar, X. Yuan, S. Li, B. Le Guennic, J. Ma, C. Zhang, D. Jacquemin, J. Zhao, *J. Mater. Chem. B* **2014**, *2*, 2838-2854; (b) J. Sun, F. Zhong, X. Yi, J. Zhao, *Inorg. Chem.* **2013**, *52*, 6299–6310; (c) J. Wang, Y. Lu, N. McGoldrick, C. Zhang, W. Yang, J. Zhao, S.M. Draper, . *Mater. Chem. C* **2016**, *4*, 6131-6139 (d) C. E. McCusker, D. Hablot, R. Ziessel, F. N. Castellano, *Inorg. Chem.* **2012**, *51*, 7957–7959

[4] (a) S. P.-Y. Li, C. T.-S. Lau, M.-W. Louie, Y.-W. Lam, S. H. Cheng, K. K.-W. Lo, *Biomaterials* **2013**, *34*, 7519–7532; (b) R. Gao, D. G. Ho, B. Hernandez, M. Selke, D. Murphy, P. I. Djurovich, M. E. Thompson, *J. Am. Chem. Soc.* **2002**, *124*, 14828–14829.

[5] (a) P. I. Djurovich, D. Murphy, M. E. Thompson, B. Hernandez, R. Gao, P. L. Hunt, M. Selke, *Dalton Trans.* **2007**, *34*, 3763–3770; (b) S. Lamansky, P. Djurovich, D. Murphy, F. Abdel-Razzaq, R. Kwong, I. Tsyba, M. Bortz, B. Mui, R. Bau, M. E. Thompson, *Inorg. Chem.* **2001**, *40*, 1704–1711.

[6] B. D. Gutiérrez-Ramos, J. Bañuelos, T. Arbeloa, I. López Arbeloa, P. E. González-Navarro, K. Wrobel, L. Cerdán, I. García-Moreno, A. Costela, E. Peña-Cabrera, *Chem.- Eur. J.* **2015**, *21*, 1755–1764.

[7] N. Boens, B. Verbelen, W. Dehaen, *Eur. J. Org. Chem.* **2015**, 6577-6595 and references cited therein.

[8] P. Coppo, E. A. Plummer, L. De Cola, *Chem. Commun*. **2004**, 1774-1775.

[9] G. Durán-Sampedro, A. R. Agarrabeitia, L. Cerdán, M. E. Pérez-Ojeda, A. Costela, I. García-Moreno, I. Esnal, J. Bañuelos, I. López Arbeloa, M J. Ortiz, *Adv. Funct. Mater.* **2013**, *23*, 4195–4205.

[10] A. Poirel, P. Retailleau, A. De Nicola, R. Ziessel, *Chem.- Eur. J.* **2014**, *20*, 1252–1257.

[11] (a) E. M. Sánchez-Carnerero, L. Gartzia-Rivero, F. Moreno, B. L. Maroto, A. R. Agarrabeitia, M. J. Ortiz, J. Bañuelos, Í. López-Arbeloa, S. de la Moya, *Chem. Commun.* **2014**, *50*, 12765–12767; (b) E. M. Sánchez-Carnerero, F. Moreno, B. L. Maroto, A. R. Agarrabeitia, M. J. Ortiz, B. G. Vo, G. Muller, S. de la Moya, *J. Am. Chem. Soc.* **2014**, *136*, 3346–3349.

[12] Y. Gabe, Y. Urano, K. Kikuchi, H. Kojima, T. Nagano, *J. Am. Chem. Soc.* **2004**, *126*, 3357-3367.

[13] Y. Chen, J. Zhao, H. Guo, L. Xie, *J. Org. Chem.* **2012**, *77*, 2192–2206.

[14] (a) A. A. Rachford, R. Ziessel, T. Bura, P. Retailleau, F. N. Castellano, *Inorg. Chem.* **2010**, *49*, 3730–3736; (b) H. A. Montejano, F. Amat-Guerri, A. Costela, I. García-Moreno, M. Liras, R. Sastre, *J. Photochem. Photobiol. A Chem.* **2006**, *181*, 142–146; (c) M. Galletta, S. Campagna, M. Quesada, G. Ulrich, R. Ziessel, *Chem. Commun.* **2005**, 4222–4224.
[15] B. Turfan, E. U. Akkaya, *Org. Lett.* **2002**, *4*, 2857–2859.
[16] T. Mosmann, *J. Immunol. Methods* **1983**, *65*, 55-63.
[17] C. Marti, O. Jürgens, O. Cuenca, M. Casals, S. Nonell, *J. Photochem. Photobiol A,* **1996**, *97,* 11-18.
[18] N. Epelde-Elezcano, V. Martínez-Martínez, E. Peña-Cabrera, C. F. A. Gómez-Durán, I. López Arbeloa, S. Lacombe, *RSC Adv.* **2016**, *6*, 41991–41998.
[19] M. J. Frisch, G. W. Trucks, H. B. Schlegel, G. E. Scuseria, M. A. Robb, J. R. Cheeseman, G. Scalmani, V. Barone, B. Mennucci, G. A. Petersson, H. Nakatsuji, M. Caricato, X. Li, H. P. Hratchian, A. F. Izmaylov, J. Bloino, G. Zheng, J. L. Sonnenberg, M. Hada, M. Ehara, K. Toyota, R. Fukuda, J. Hasegawa, M. Ishida, T. Nakajima, Y. Honda, O. Kitao, H. Nakai, T. Vreven, J. A. Montgomery, J. E. Peralta, F. Ogliaro, M. Bearpark, J. J. Heyd, E. Brothers, K. N. Kudin, V. N. Staroverov, R. Kobayashi, J. Normand, K. Raghavachari, A. Rendell, J. C. Burant, S. S. Iyengar, J. Tomasi, M. Cossi, N. Rega, J. M. Millam, M. Klene, J. E. Knox, J. B. Cross, V. Bakken, C. Adamo, J. Jaramillo, R. Gomperts, R. E. Stratmann, O. Yazyev, A. J. Austin, R. Cammi, C. Pomelli, J. W. Ochterski, R. L. Martin, K. Morokuma, V. G. Zakrzewski, G. A. Voth, P. Salvador, J. J. Dannenberg, S. Dapprich, A. D. Daniels, Farkas, J. B. Foresman, J. V Ortiz, J. Cioslowski, D. J. Fox, *Gaussian 09, Revis. B.01,* Gaussian, Inc., Wallingford CT, **2009**.

10.1002/chem.201701347

WILEY-VCH

Entry for the Table of Contents (Please choose one layout)

Layout 1:

FULL PAPER

Text for Table of Contents

New BODIPY-Iridium(III) complexes, synthesized by a straightforward synthetic approach, exhibit efficient singlet oxygen generation, low dark and high photo-cytoxicity under visible radiation even at low PS concentrations.

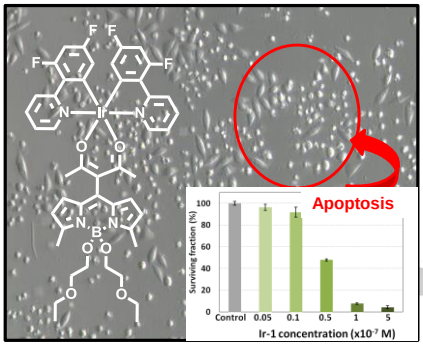

E. Palao, R. Sola-Llano, A. Tabero, H. Manzano, A. R. Agarrabeitia, A. Villanueva, I. López-Arbeloa, V. Martínez-Martínez, and M. J. Ortiz**

Page No. – Page No.

AcetylacetonateBODIPY−biscyclometalated Iridium(III) complexes: Effective strategy towards smarter fluorescent-photosensitizer agents

Layout 2:

FULL PAPER

((Insert TOC Graphic here; max. width: 11.5 cm; max. height: 2.5 cm))

Page No. – Page No.

Title

Text for Table of Contents